Direct determination of the zero-field splitting for a single

Direct determination of the zero-field splitting for a single Co^{2+} ion embedded in a CdTe/ZnTe quantum dot

J. Kobak,[1,*] A. Bogucki,[1] T. Smoleński,[1] M. Papaj,[1,2] M. Koperski,[1,3] M. Potemski,[3] P. Kossacki,[1] A. Golnik,[1] and W. Pacuski[1]

[1]*Institute of Experimental Physics, Faculty of Physics, University of Warsaw, ul. Pasteura 5, 02-093 Warsaw, Poland*

[2]*Department of Physics, Massachusetts Institute of Technology, Cambridge, Massachusetts 02139, USA*

[3]*Laboratoire National des Champs Magnétiques Intenses, CNRS-UGA-UPS-INSA-EMFL, 30942 Grenoble, France*

(Received 24 October 2016; published 23 January 2018)

When a Co^{2+} impurity is embedded in a semiconductor structure, crystal strain strongly influences the zero-field splitting between Co^{2+} states with spin projection $S_z = \pm 3/2$ and $S_z = \pm 1/2$. Experimental evidence of this effect has been given in previous studies; however, direct measurement of the strain-induced zero-field splitting has been inaccessible so far. Here this splitting is determined thanks to magneto-optical studies of an individual Co^{2+} ion in an epitaxial CdTe quantum dot in a ZnTe barrier. Using partially allowed optical transitions, we measure the strain-induced zero-field splitting of the Co^{2+} ion directly in the excitonic photoluminescence spectrum. Moreover, by observation of anticrossing of $S_z = +3/2$ and $S_z = -1/2$ Co^{2+} spin states in a magnetic field, we determine the axial and in-plane components of the crystal field acting on the Co^{2+}. The proposed technique can be applied to optical determination of the zero-field splitting of other transition-metal ions in quantum dots.

DOI: 10.1103/PhysRevB.97.045305

I. INTRODUCTION

The first observation of excitonic emission from a quantum dot (QD) with a single Co^{2+} ion [1] led to the discovery that a quantum dot containing a single magnetic ion exhibits efficient radiative excitonic recombination, even when the recombination energy is higher than the intraionic transition of the magnetic ion. Therefore, optical manipulation of a single magnetic ion spin is possible not only in classical systems with a single Mn^{2+} ion in QDs with a relatively low energy gap, CdTe/ZnTe [2–6] and InAs/GaAs [7–9], but also in QDs with a higher-energy gap such as CdSe/ZnSe [1,10–12] or in QD systems doped with impurities considered previously as killers of photoluminescence: Co^{2+} [1], Fe^{2+} [13,14], and Cr^{2+} [15,16]. For all the systems studied so far it has been found that the ground state of the magnetic ion is significantly influenced by the local strain present in a quantum dot. Such an effect is of particular importance for future applications in solotronics (optoelectronics based on single dopants [17]) and spintronics based on magnetic QDs [18–28]. The effect of strain may be demonstrated as beating in the coherent precession of the single magnetic ion spin [29], as changes of occupation and energy of levels corresponding to various projections of the ion spin [1,7,15], or even as a change in the character of the Fe^{2+} ion ground state, from nonmagnetic in bulk to magnetic in a QD [13]. However, so far only indirect methods have been used to estimate the strain-induced zero-field splitting of single magnetic ions in QDs: from the depolarization efficiency of an optically oriented ion [4], from photoluminescence (PL) peak line shape [30], from the variation of the coherent oscillation amplitude [29,31], and from the relative PL peak intensity of lines corresponding to various spin projections [1,7,13,15]. Here we present a method for the measurement of the strain-induced zero-field splitting of a magnetic ion directly by observation of the corresponding splitting in the exciton photoluminescence spectrum. We apply this method to a precise determination of the zero-field splitting of Co^{2+} in a CdTe/ZnTe QD.

This paper is organized in the following way: first, we give experimental details, and we recall a typical spectrum of the neutral exciton in a QD with a single Co^{2+} ion. Next, we introduce partially allowed transitions which are used to determine the zero-field splitting of a single Co^{2+} ion in a QD. Finally, we present the magneto-optical effects of anticrossing of Co^{2+} spin states. From this anticrossing we determine the Hamiltonian parameters D and E representing the axial and in-plane components of the crystal field.

II. SAMPLES AND EXPERIMENTAL SETUP

We studied two similar structures with ZnTe barriers and CdTe QDs doped with Co^{2+} ions. The growth of the investigated structures was performed by molecular beam epitaxy on a GaAs (100)-oriented substrate. Formation of the QDs was induced by the amorphous Te desorption method [32]. During the CdTe deposition process we introduced low-level δ-doping with Co^{2+} ions using a high-temperature effusion cell working at 1200 °C. Since the molecular fluxes of cobalt used during the growth of the QDs are smaller than the accuracy of the vacuum gauge, for both investigated structures we fabricated the reference $Zn_{1-x}Co_xTe$ layers grown under the same Co^{2+} flux. Such layers of diluted magnetic semiconductor allowed us to determine precisely the Co^{2+} concentration x by measuring the giant Zeeman effect (for more detail see [33,34]). The final Co^{2+} concentration in the reference samples was found to be equal to about 0.3%. The same concentration was therefore expected in the thin $Cd_{1-x}Co_xTe$ layer before transformation into QDs.

*Jakub.Kobak@fuw.edu.pl

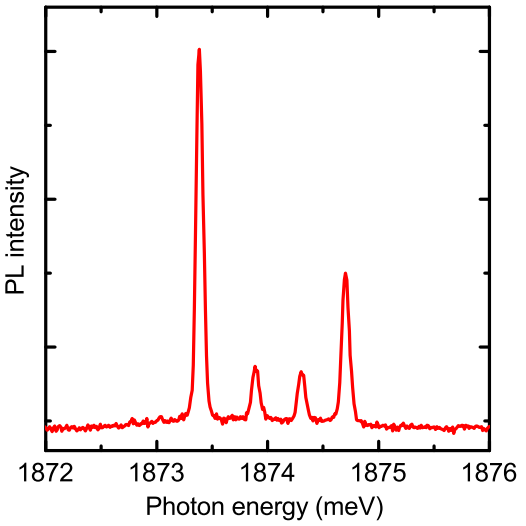

FIG. 1. Typical photoluminescence spectrum of a neutral exciton in a CdTe/ZnTe QD with a single Co^{2+} ion at $T = 3$ K. This Co^{2+} ion has a ground state with spin projection $\pm 3/2$, and as a consequence, the outer lines related to such spin states are much more pronounced than the inner emission lines related to the $\pm 1/2$ states.

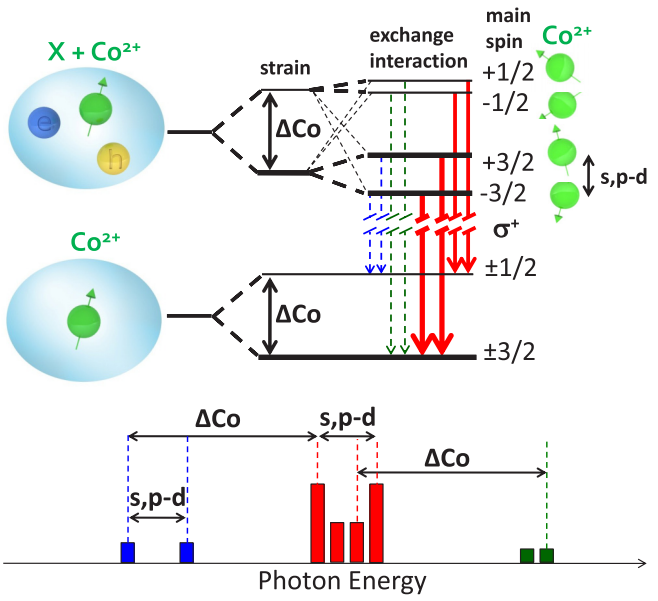

FIG. 2. Schematic diagram of the zero-field optical transitions between the energy levels of a singly Co^{2+}-doped quantum dot with and without a neutral exciton. Numbers indicate the main Co^{2+} spin wave function. Red solid arrows denote the transitions for which Co^{2+} spin is conserved: the only allowed optical transitions of a bright exciton if the Co^{2+} states are pure. Blue and green dashed arrows denote transitions partially allowed due to Co^{2+} spin-state mixing. The energy differences between the strongest emission lines in the spectrum (red outer lines) and the weak, partially allowed lines at lower energy (blue lines) are exactly equal to the cobalt zero-field splitting Δ_{Co}.

The maximum compressive strain in our QDs is related to the lattice mismatch of about 6% defined by the lattice constants of CdTe ($a = 6.48$ Å) and ZnTe ($a = 6.10$ Å). In practice, the strain can be lower due to intermixing of Zn and Cd between the QDs and the barrier or due to partial relaxation of the two-monolayer-thick CdTe layer during formation of the QDs.

For the microphotoluminescence experiments the samples were immersed in liquid helium inside a magneto-optical bath cryostat with a magnetic field of up to 10 T. The measurements were performed at a temperature of about 1.5 K using a high-resolution reflective microscope, which results in a laser spot of about 0.5 μm diameter. This experimental setup allowed us to study the optical properties of well-separated emission lines in magnetic fields with a polarization resolution. Complementary studies requiring a high magnetic field were performed at the Grenoble High Magnetic Field Laboratory, where samples were immersed in helium gas at $T = 10$ K inside a 20-MW resistive magnet producing a magnetic field of up to 28 T.

III. RESULTS

A. Typical photoluminescence spectrum of a QD with a single Co^{2+} ion

Figure 1 presents a photoluminescence spectrum of a bright neutral exciton in a CdTe/ZnTe QD with a single Co^{2+} ion in zero magnetic field. Emission is split due to the s, p-d exchange interaction between the exciton and the magnetic ion. The four observed lines result from the four possible spin projections of a Co^{2+} ion with spin 3/2 onto the quantization axis given by the heavy-hole exciton in the QD [1]. More precisely, in an excited state formed by an exciton and a Co^{2+} ion, for each projection of excitonic spin (± 1, corresponding to σ^+ and σ^- circular polarizations) there are four energy levels, and in the final state after exciton recombination there are four quantum states (two doubly degenerate levels at zero field) of Co^{2+}. In each circular polarization there are 16 possible transitions, but only 4 are optically allowed due to the requirement of Co^{2+} spin conservation for an electric dipole transition (solid arrows in Fig. 2). In zero magnetic field the four lines for σ^+ polarization coincide with those for σ^-.

The intensity of the two inner and two outer lines reflects the differences in occupancy of the various Co^{2+} states. Figure 1 shows a typical case, in which the cobalt has a ground state with spin projection $\pm 3/2$ and, consequently, the outer lines related to such spin states are more pronounced than the lines related to the $\pm 1/2$ states (inner lines). However, we argue that apart from the Co^{2+} level ordering, such main lines do not carry sufficient information about the absolute value of the Co^{2+} zero-field splitting. This is because the line separation energy is determined by the s, p-d exchange interaction and not by the splitting of the Co^{2+} states. Moreover, the occupancy of the various states of Co^{2+} under optical excitation is not governed simply by the temperature and the Boltzmann distribution. One could try to describe it by an effective temperature, but there is no good method to determine such a parameter, which could be an order of magnitude larger than the actual experimental temperature (e.g., 10 or 30 K instead of 1.7 K in the Supplementary Information of Ref. [1]). Moreover, Fig. 1 shows that the two outer lines of a QD with a single Co^{2+} ion

exhibit unequal intensity, which is a fingerprint of efficient relaxation of the Co^{2+}-exciton system during the lifetime of a single exciton introduced to the QD. This makes the measurement of the occupancy distribution of Co^{2+} states in an empty dot even more complex. Therefore, we conclude that precise determination of the Co^{2+} zero-field splitting from an analysis of the four main photoemission lines of a QD with a single Co^{2+} is not feasible.

B. Partially allowed transitions and determination of the Co^{2+} zero-field splitting

In the previous section we discussed the four main optical transitions with conserved spin of the Co^{2+} ion. In this section we report the additional bright-neutral-exciton transitions, which can be observed only if in-plane strain mixes Co^{2+} spin states. Since such mixing is influenced by the s,p-d exchange interaction between the carriers and the magnetic ion, Co^{2+} spin mixing is slightly different for a QD with and without an exciton. When the spin wave function of Co^{2+} is not identical in the initial and final states of the optical transition, part of the oscillator strength is distributed between transitions where the main spin component is different in the initial and final states but both states are not fully orthogonal. This effect opens the possibility of studying partially allowed optical transitions, shown by the blue and green dashed arrows in Fig. 2. The intensity of such emission lines is strongly sensitive to the parameters describing the Co^{2+} ion. For the values of the parameters determined in this work, the intensity ratio between the main emission lines (colored red in Fig. 2) and the partially allowed lines (colored blue and green in Fig. 2) is three orders of magnitude. Measurements of such weak PL lines is experimentally challenging, but they are worth the effort because the partially allowed lines carry information about the parameters describing the spin structure of the Co^{2+} ion. In particular, the energy differences between the strongest emission lines in the spectra (red outer lines) and the weak, partially allowed lines at lower energy (blue lines) are exactly equal to the cobalt spin-state splitting Δ_{Co} since such transitions have the same initial states ($\pm 3/2$ with an admixture of $\mp 1/2$) but different final states ($\pm 3/2$ with an admixture of $\mp 1/2$ and $\pm 1/2$ with an admixture of $\mp 3/2$, respectively). The same energy distance (Δ_{Co}) occurs between the inner main lines (red) and the partially allowed emission lines at higher energy (green). Note that the intensity of these lines should be much weaker than that of the already weak lines on the low-energy side. The intensity ratio of the green and blue lines should be the same as the ratio of the outer and inner lines from the strong (allowed) lines. Therefore, in most experiments we do not observe such lines (e.g., for the particular QD presented in Fig. 3). The energy splitting of the low-energy weak emission lines (blue) is related to the s,p-d exchange interaction in the initial state, so it is the same as the splitting of the outer main emission lines (red). Similarly, the high-energy weak emission lines (green) exhibit splitting equal to the splitting of the inner main lines (red).

Experimental observation of partially allowed transitions is shown in Fig. 3(a), which presents typical low-temperature magnetophotoluminescence of a bright exciton in a QD with a single Co^{2+} ion in the Faraday configuration, measured in two circular polarizations of detection. Line identification on the spectrum is in agreement with the simulation shown in Fig. 3(b). In both Figs. 3(a) and 3(b) we observe strong main emission lines [red lines in Fig. 3(b) or the scheme in Fig. 2] corresponding to transitions with conserved Co^{2+} spin. We additionally observe three weak emission lines. The first one is associated with the dark-exciton recombination [black line in Fig. 3(b)], which involves a change in the Co^{2+} spin from mainly $+3/2$ to mainly $-3/2$, so it exhibits the largest g factor and is a fingerprint of Co^{2+} spin-state mixing, but it does not carry information about the zero-field splitting of Co^{2+}. Two more weak lines are related to bright-exciton transitions partially allowed by cobalt $\pm 3/2$ and $\mp 1/2$ spin-state mixing [blue lines in Fig. 3(b) and the scheme in Fig. 2]. We determine the zero-field splitting of cobalt ($\Delta_{Co} = 3.13$ meV for Co^{2+} shown in Fig. 3) by subtraction of the emission energies of the lines related to the transitions for which the initial state is the same (mainly $\pm 3/2$) but the final state is different (mainly $\pm 3/2$ and $\mp 1/2$ for weak and strong lines, respectively). Note that the values of the Δ_{Co} parameter estimated from the two pairs of emission lines are the same.

The simulation presented in Fig. 3(b) is based on a simple model of the exciton-Co^{2+}-ion system described in detail in the Methods section of Ref. [1]. The most important part of our theoretical description is given by the standard Hamiltonian of the Co^{2+} ion, which is also the Hamiltonian of the final state of the system after the exciton recombination:

$$\mathcal{H}_{Co} = g_{Co}\mu_B \vec{\mathbf{B}} \cdot \vec{\mathbf{J}} + D\mathbf{J}_z^2 + E(\mathbf{J}_y^2 - \mathbf{J}_x^2), \qquad (1)$$

where the first term represents the Zeeman effect described by the magnetic ion g factor, Bohr magneton μ_B, magnetic field $\vec{\mathbf{B}}$, and the total magnetic momentum $\vec{\mathbf{J}}$ ($J = 3/2$). The second and third terms describe the magnetic anisotropy of a magnetic impurity, with D and E representing the axial and in-plane components of the crystal field. Both parameters D and E can be determined based on the anticrossings discussed in detail in the next section.

C. Anticrossing of Co^{2+} ion spin states and determination of crystal-field parameters

Since the g factors are different for the main and partially allowed transitions (see Fig. 3), approaching various lines in a magnetic field is inevitable. A series of anticrossings between the main and partially allowed transitions is observed in the magnetophotoluminescence experiment shown in Fig. 4(a). Additionally, Fig. 4(b) presents a corresponding simulation of the optical spectra, and Fig. 4(c) presents simulated energy levels of a neutral exciton in a CdTe QD with Co^{2+} (initial states of photoluminescence) and an empty dot with a single cobalt ion (final states). All panels of Fig. 4 show important spectral features closely related to the spin structure of the Co^{2+} ion. Anticrossing between $+3/2$ and $-1/2$ cobalt spin states in the absence of an exciton appears four times in the excitonic spectra (due to the final state of recombination); all appearances are at the same magnetic field [about 7.5 T for the QD in Fig. 4(a)]. They are denoted in Figs. 4(b) and 4(c) by black circles. Red and blue squares in Figs. 4(b) and 4(c) represent anticrossings of cobalt spin states modified by the presence of carriers forming a neutral exciton, which acts on

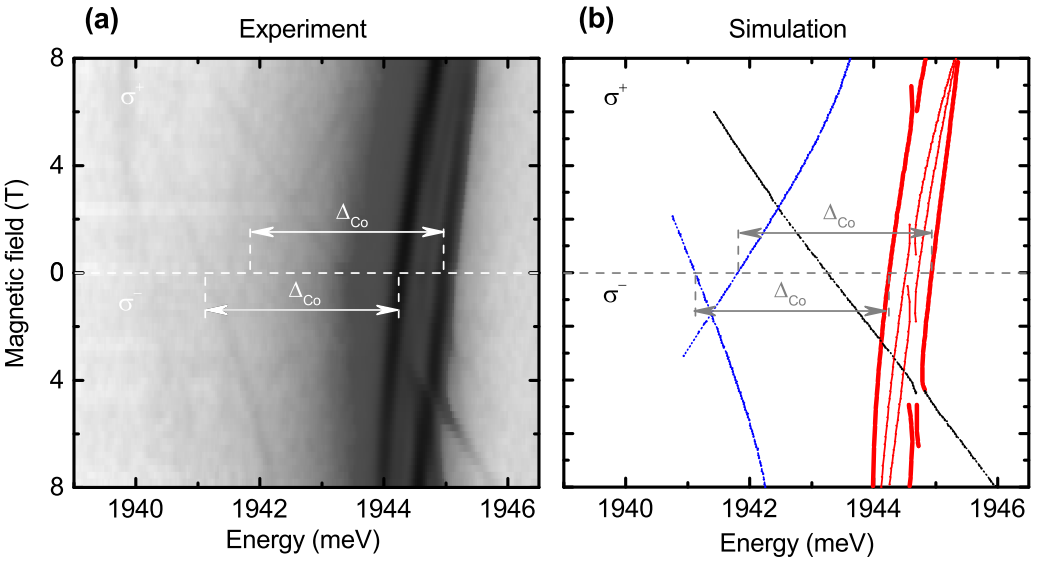

FIG. 3. (a) Polarization-resolved PL intensity map of a neutral exciton in a CdTe/ZnTe QD with a single Co^{2+} ion as a function of the magnetic field in the Faraday configuration at $T = 1.5$ K. (b) Corresponding simulation of the optical transitions with the model described in the text. There are four main emission lines [red lines in (b)] corresponding to the bright-exciton transition with conserved spin of Co^{2+} and three weak emission lines: one associated with the dark-exciton recombination [black line in (b)] which does not carry information about the zero-field splitting and two lines related to the transitions allowed by cobalt $\pm 3/2$ and $\mp 1/2$ spin-state mixing [blue lines in (b)]. As explained in Fig. 2, the zero-field splitting of cobalt ($\Delta_{Co} = 3.13$ meV) is determined by subtraction of the energies for pairs of transitions for which the initial state is the same ($\pm 3/2$) but the final state is different ($\pm 3/2$ and $\mp 1/2$). The values of the Δ_{Co} parameter estimated from two pairs of emission lines are the same.

the Co^{2+} as an effective magnetic field of about 3 T for the QD in Fig. 4(a). As a consequence, such anticrossings are shifted and are visible at about 4.5 and 10.5 T for σ^+ and σ^- polarizations of detection, respectively. The observed shift is analogous to the shift of the magnetic ion levels anticrossing from zero field to a field of about 2 T, which has already been reported for the Mn^{2+} + h complex in InAs/GaAs QDs [7–9] and for Fe^{2+} in CdSe/ZnSe QDs [13], where s, p-d exchange interaction with the exciton also acted on the magnetic ion as an effective magnetic field.

Particularly important for this work are the anticrossings in the final state which are marked in Fig. 4 by black circles. They give additional information about Co^{2+} properties in the absence of carriers. In such an anticrossing the separation

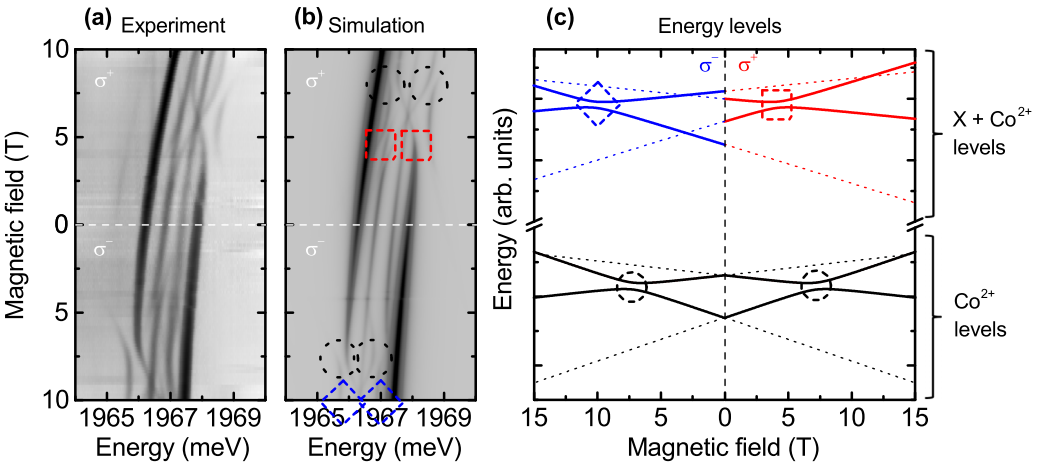

FIG. 4. (a) Polarization-resolved magneto-PL intensity map in the Faraday configuration at $T = 1.5$ K for a CdTe/ZnTe QD with a single Co^{2+} ion exhibiting within the experimental range an anticrossing of 3/2 and $-1/2$ spin states. (b) Corresponding simulation of the optical spectra. (c) Corresponding simulation of the energies of the initial state (exciton plus Co^{2+} system) and final state (empty dot with a single Co^{2+} ion) of the optical transition. Anticrossing between $+3/2$ and $-1/2$ cobalt spin states in the absence of an exciton appears four times in the spectra, at a magnetic field of about 7.5 T, and is denoted in (b) and (c) by black circles. Red and blue squares in (b) and (c) represent anticrossings of cobalt spin states modified by the presence of a neutral exciton which acts on Co^{2+} as an effective magnetic field. As a consequence, such anticrossings are shifted to about 4.5 and 10.5 T for σ^+ and σ^- polarizations, respectively.

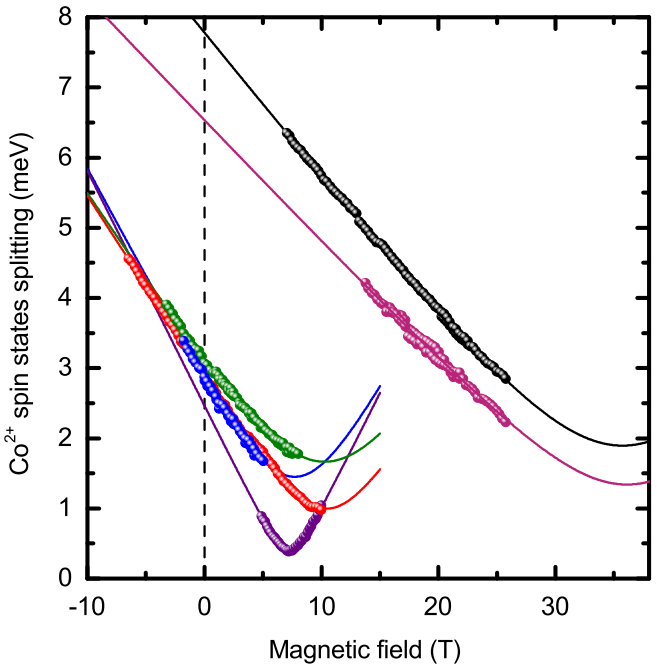

FIG. 5. Points: energy difference between mixed $\pm 3/2$ and $\mp 1/2$ spin states of various Co^{2+} ions in CdTe/ZnTe QDs, determined from PL spectra as a function of the magnetic field, near the anticrossing. Solid lines: fit to the Co^{2+} state splitting given by Eq. (2) with the fitting parameters summarized in Table I.

energy of the spectral lines corresponds directly to the separation energy between the Co^{2+} states close to the anticrossing of spin states $+3/2$ and $-1/2$. In Fig. 5 we plot the dependence of the splitting of such Co^{2+} spin states $\Delta_{Co}(B)$ as a function of the magnetic field for the QDs shown in Fig. 3 (violet points) and Fig. 4 (green points) and for four other QDs with a single Co^{2+} ion.

Solving Hamiltonian (1) leads us to an analytical formula describing the evolution of the energy distance between mixed $\pm 3/2$ and $\mp 1/2$ spin states of Co^{2+} with magnetic field:

$$\Delta_{Co}(B) = 2\sqrt{3E^2 + (g_{ion}\mu_B B + D)^2}, \qquad (2)$$

where the parameters D and E (the axial and in-plane components of the crystal field) can be extracted directly from the experimental data. Parameter E can be determined from the value of Δ_{Co} for the magnetic field at which anticrossing between $+3/2$ and $-1/2$ spin states appears [$\Delta_{Co}(B_{min\Delta}) = 2\sqrt{3}E$]. Knowing E, one can obtain D from the zero-field spin-state splitting given by the formula $\Delta_{Co}(0) = 2\sqrt{3E^2 + D^2}$. Finally, the g factor is equal to $-D/(\mu_B B_{min\Delta})$. Parameters D, E, and the g factor of the Co^{2+} ion can also be determined by fitting Eq. (2) to the experimental data, as shown by the solid lines in Fig. 5.

The values of the parameters describing Co^{2+} ions in all the studied QDs are summarized in Table I. The data are sorted in increasing order with respect to the zero-field splitting Δ_{Co}, which varies from about 2.5 to almost 8 meV. The value of the parameter D is in the range between -1.22 and -3.77 meV. For all the discussed QDs the parameter D is negative, which favors states of spin equal to $\pm 3/2$. Parameter E, which causes the mixing of Co^{2+} spin states, varies from 0.12 to 0.6 meV.

TABLE I. Values of key parameters describing the spin configuration and anisotropy of the Co^{2+} ion for all studied QDs: zero-field splitting $\Delta_{Co}(0)$, axial (D) and in-plane (E) components of the crystal field, and g_{Co}. Measurements of the two largest zero-field splittings (the last two rows) had to be performed at the high-magnetic-field laboratory in Grenoble.

$\Delta_{Co}(0)$ (meV)	D (meV)	E (meV)	g_{Co}
2.47	-1.22 ± 0.02	0.12 ± 0.01	2.91 ± 0.06
2.86	-1.23 ± 0.08	0.42 ± 0.08	2.8 ± 0.3
2.91	-1.37 ± 0.02	0.29 ± 0.02	2.27 ± 0.04
3.13	-1.33 ± 0.03	0.48 ± 0.02	2.2 ± 0.1
6.53	-3.2 ± 0.1	0.4 ± 0.2	1.6 ± 0.3
7.78	-3.8 ± 0.1	0.6 ± 0.1	1.8 ± 0.1

The values of the Co^{2+} g factor strongly differ from each other, starting from 1.6 and ending with a value of 2.91. Analysis of Table I shows that there is an anticorrelation between Δ_{Co} and g_{Co}. The smaller the Co^{2+} zero-field splitting is, the larger the value of the $Co^{2+}g$ factor is. Surprisingly, for declining values of the Co^{2+} zero-field splitting we do not observe the convergence of the Landé factor of Co^{2+} to the limit defined by an unstrained CdTe crystal [35], which is equal to 2.31. This shows that there are other important factors affecting the structure of the energy states of the cobalt ion. One of the possible explanations of a g factor lower than 2.31 is that a larger g factor would be observed for axes other than the growth axis tested in our experiment.

We note that the distribution of the measured values of the zero-field splitting is probably not governed by the distribution in the studied samples but is rather affected by the preselection of the studied Co^{2+} ions caused by our experimental limitations. At zero field or at a magnetic field in the range of a few teslas, only relatively small zero-field splitting of Co^{2+} can be determined. For large zero-field splitting partially allowed transitions are too weak to be observed. Therefore, we expect that the real distribution of the Co^{2+} zero-field splitting in the samples is even wider than observed and that a typical value is larger than about 3 meV, observed a few times in our first experiments. This expectation is supported by the high-magnetic-field experiments (claret and black data in Fig. 5), where anticrossings of $+3/2$ and $-1/2$ are expected at about 35 T for a Co^{2+} ion with $\Delta_{Co}(0)$ equal to almost 7 and 8 meV, respectively.

The absolute values of the parameter D obtained in this work are significantly larger than the values reported for semiconductor systems without strain. For Co^{2+} in zinc-blende semiconductors like CdTe, ZnTe, and ZnSe the parameter D is neglected [35–37]. In wurtzite-structure diluted magnetic semiconductors with Co^{2+} the parameter D was found to be positive, with the absolute value one order of magnitude smaller than in our experiments on QDs: +0.06 meV for CdSe [38,39], +0.08 meV for CdS [38,40], and +0.34 meV for ZnO [41–47]. This result is consistent with the fact that crystal distortion describing the difference between the zinc blend and the wurtzite structure is one order of magnitude smaller (e.g., for ZnO) than the distortion induced by 6% of the lattice mismatch between the material of the quantum dot and the

barrier. The large dispersion in the values of the parameter D and other parameters observed for our QDs (Table I) can be understood as a consequence of partial relaxation during formation of the QDs, which can lead both to the release of the total strain and to the inhomogeneous distribution of the strain within QDs [48,49]. Since the Co^{2+} ion probes only very local strain, ions placed in various positions within the dot or in various dots can exhibit significantly different strain.

In strained semiconductor systems, the parameter D obtained in this work for Co^{2+} can be compared to values obtained for other transition-metal ions. For the Mn^{2+} ions embedded in CdTe/ZnTe QDs, the parameter $D \approx 0.007$ meV was determined from the depolarization efficiency of optically oriented ions [4] and from the variation of the coherent oscillation amplitude [29], which were also used for the determination of the parameter $E = 1.8\,\mu$eV [15]. Much larger values, in the range of meV, are expected from the magnetophotoluminescence of the main emission lines in QDs with transition-metal ions exhibiting nonzero orbital momentum, $D > 0.8$ meV [13] for Fe^{2+} and $D > 2.25$ meV [15] for Cr^{2+}. Finally, in our first report on the main emission lines of the QD CdTe/ZnTe with a single Co^{2+} ion, using a multiparameter fit, we obtained the value $D_z \approx -1.4$ meV [1] in the same range as the directly determined values presented in this work.

IV. CONCLUSIONS

We have presented optical studies of individual Co^{2+} ions in epitaxial QDs. Using partially allowed optical transitions, we described the strain-induced zero-field splitting of Co^{2+} ions and anticrossing of Co^{2+} spin states. From this anticrossing we determined the Hamiltonian parameters D and E representing the axial and in-plane components of the crystal field. Our technique can be applied to optical measurements of the zero-field splitting of other transition-metal ions (e.g., Cr^{2+}, Fe^{2+}) in QDs, provided that very low noise spectra or high enough magnetic fields are available.

ACKNOWLEDGMENTS

This work was partially supported by the Polish National Science Centre under Decisions No. DEC-2015/18/E/ST3/00559, No. DEC-2016/23/B/ST3/03437, No. DEC-2011/02/A/ST3/00131, No. DEC-2013/09/B/ST3/02603, and No. DEC-2012/05/N/ST3/03209 and by the Polish Ministry of Science and Higher Education program Iuventus Plus in the years 2015–2017, Project No. IP2014 034573, and in the years 2013–2017 as the research grant "Diamentowy Grant." Three of us (J.K., T.S., and M.K.) were supported by the Polish National Science Centre through Ph.D. scholarship grants under Decisions No. DEC-2015/16/T/ST3/00371, No. DEC-2016/20/T/ST3/00028, and No. DEC-2015/16/T/ST3/00497. Two of us (J.K. and T.S.) were supported by the Foundation for Polish Science through the START program. The project was carried out with the use of CePT, CeZaMat, and NLTK infrastructures financed by the European Union: the European Regional Development Fund within the Operational Programme "Innovative economy."

[1] J. Kobak, T. Smoleński, M. Goryca, M. Papaj, K. Gietka, A. Bogucki, M. Koperski, J.-G. Rousset, J. Suffczyński, E. Janik, M. Nawrocki, A. Golnik, P. Kossacki, and W. Pacuski, Designing quantum dots for solotronics, Nat. Commun. **5**, 3191 (2014).

[2] L. Besombes, Y. Léger, L. Maingault, D. Ferrand, H. Mariette, and J. Cibert, Probing the Spin State of a Single Magnetic Ion in an Individual Quantum Dot, Phys. Rev. Lett. **93**, 207403 (2004).

[3] L. Besombes, Y. Leger, L. Maingault, D. Ferrand, H. Mariette, and J. Cibert, Carrier-induced spin splitting of an individual magnetic atom embedded in a quantum dot, Phys. Rev. B **71**, 161307 (2005).

[4] C. Le Gall, L. Besombes, H. Boukari, R. Kolodka, J. Cibert, and H. Mariette, Optical Spin Orientation of a Single Manganese Atom in a Semiconductor Quantum Dot Using Quasiresonant Photoexcitation, Phys. Rev. Lett. **102**, 127402 (2009).

[5] M. Goryca, T. Kazimierczuk, M. Nawrocki, A. Golnik, J. A. Gaj, P. Kossacki, P. Wojnar, and G. Karczewski, Optical Manipulation of a Single Mn Spin in a CdTe-Based Quantum Dot, Phys. Rev. Lett. **103**, 087401 (2009).

[6] M. Goryca, P. Plochocka, T. Kazimierczuk, P. Wojnar, G. Karczewski, J. A. Gaj, M. Potemski, and P. Kossacki, Brightening of dark excitons in a single CdTe quantum dot containing a single Mn^{2+} ion, Phys. Rev. B **82**, 165323 (2010).

[7] A. Kudelski, A. Lemaître, A. Miard, P. Voisin, T. C. M. Graham, R. J. Warburton, and O. Krebs, Optically Probing the Fine Structure of a Single Mn Atom in an InAs Quantum Dot, Phys. Rev. Lett. **99**, 247209 (2007).

[8] O. Krebs, E. Benjamin, and A. Lemaître, Magnetic anisotropy of singly Mn-doped InAs/GaAs quantum dots, Phys. Rev. B **80**, 165315 (2009).

[9] E. Baudin, E. Benjamin, A. Lemaître, and O. Krebs, Optical Pumping and a Nondestructive Readout of a Single Magnetic Impurity Spin in an InAs/GaAs Quantum Dot, Phys. Rev. Lett. **107**, 197402 (2011).

[10] T. Smoleński, W. Pacuski, M. Goryca, M. Nawrocki, A. Golnik, and P. Kossacki, Optical spin orientation of an individual Mn^{2+} ion in a CdSe/ZnSe quantum dot, Phys. Rev. B **91**, 045306 (2015).

[11] R. Fainblat, C. J. Barrows, E. Hopmann, S. Siebeneicher, V. A. Vlaskin, D. R. Gamelin, and G. Bacher, Giant excitonic exchange splittings at zero field in single colloidal cdse quantum dots doped with individual Mn^{2+} impurities, Nano Lett. **16**, 6371 (2016).

[12] K. Oreszczuk, M. Goryca, W. Pacuski, T. Smoleński, M. Nawrocki, and P. Kossacki, Origin of luminescence quenching in structures containing CdSe/ZnSe quantum dots with a few Mn^{2+} ions, Phys. Rev. B **96**, 205436 (2017).

[13] T. Smoleński, T. Kazimierczuk, J. Kobak, M. Goryca, A. Golnik, P. Kossacki, and W. Pacuski, Magnetic ground state of an individual Fe^{2+} ion in strained semiconductor nanostructure, Nat. Commun. **7**, 10484 (2016).

[14] T. Smoleński, T. Kazimierczuk, M. Goryca, W. Pacuski, and P. Kossacki, Fine structure of an exciton coupled to a single Fe^{2+} ion in a CdSe/ZnSe quantum dot, Phys. Rev. B **96**, 155411 (2017).

[15] A. Lafuente-Sampietro, H. Utsumi, H. Boukari, S. Kuroda, and L. Besombes, Individual Cr atom in a semiconductor quantum dot: Optical addressability and spin-strain coupling, Phys. Rev. B **93**, 161301 (2016).

[16] A. Lafuente-Sampietro, H. Utsumi, H. Boukari, S. Kuroda, and L. Besombes, Spin dynamics of an individual Cr atom in a semiconductor quantum dot under optical excitation, Appl. Phys. Lett. **109**, 053103 (2016).

[17] P. M. Koenraad and M. E. Flatte, Single dopants in semiconductors, Nat. Mater. **10**, 91 (2011).

[18] R. Beaulac, L. Schneider, P. I. Archer, G. Bacher, and D. R. Gamelin, Light-induced spontaneous magnetization in doped colloidal quantum dots, Science **325**, 973 (2009).

[19] K. M. Whitaker, M. Raskin, G. Kiliani, K. Beha, S. T. Ochsenbein, N. Janssen, M. Fonin, U. Rüdiger, A. Leitenstorfer, D. R. Gamelin, and R. Bratschitsch, Spin-on spintronics: Ultrafast electron spin dynamics in ZnO and $Zn_{1-x}Co_xO$ Sol–Gel films, Nano Lett. **11**, 3355 (2011).

[20] A. Pandey, S. Brovelli, R. Viswanatha, L. Li, J. Pietryga, V. I. Klimov, and S. Crooker, Long-lived photoinduced magnetization in copper-doped ZnSe-CdSe core-shell nanocrystals, Nat. Nanotechnol. **7**, 792 (2012).

[21] F. Qu, L. Villegas-Lelovsky, and P. C. Morais, Spin-split antibonding molecular ground state in manganese-doped quantum dot molecules, Phys. Rev. B **92**, 115445 (2015).

[22] B. Barman, R. Oszwałdowski, L. Schweidenback, A. H. Russ, J. M. Pientka, Y. Tsai, W.-C. Chou, W. C. Fan, J. R. Murphy, A. N. Cartwright, I. R. Sellers, A. G. Petukhov, I. Žutić, B. D. McCombe, and A. Petrou, Time-resolved magnetophotoluminescence studies of magnetic polaron dynamics in type-II quantum dots, Phys. Rev. B **92**, 035430 (2015).

[23] S. A. Loureço, R. S. Silva, A. C. A. Silva, and N. O. Dantas, Structural and optical properties of Co^{2+}-doped PbSe nanocrystals in chalcogenide glass matrix, J. Phys. Chem. C **119**, 13277 (2015).

[24] W. D. Rice, W. Liu, T. A. Baker, N. A. Sinitsyn, V. I. Klimov, and S. A. Crooker, Revealing giant internal magnetic fields due to spin fluctuations in magnetically doped colloidal nanocrystals, Nat. Nanotechnol. **11**, 137 (2016).

[25] S. Nistor, M. Stefan, L. Nistor, D. Ghica, and I. Vlaicu, Distribution and interaction of Mn^{2+} ions incorporated in cubic ZnS quantum dots over a broad concentration range, J. Alloys Compd. **662**, 193 (2016).

[26] V. Moldoveanu, I. V. Dinu, R. Dragomir, and B. Tanatar, Light-hole exciton mixing and dynamics in Mn-doped quantum dots, Phys. Rev. B **93**, 165421 (2016).

[27] M. Balanta, M. Brasil, F. Iikawa, U. C. Mendes, J. Brum, Y. A. Danilov, M. Dorokhin, O. Vikhrova, and B. Zvonkov, Optically controlled spin-polarization memory effect on Mn delta-doped heterostructures, Sci. Rep. **6**, 24537 (2016).

[28] F. Muckel, J. Yang, S. Lorenz, W. Baek, H. Chang, T. Hyeon, G. Bacher, and R. Fainblat, Digital doping in magic-sized CdSe clusters, ACS Nano **10**, 7135 (2016).

[29] M. Goryca, M. Koperski, P. Wojnar, T. Smoleński, T. Kazimierczuk, A. Golnik, and P. Kossacki, Coherent Precession of an Individual 5/2 Spin, Phys. Rev. Lett. **113**, 227202 (2014).

[30] L. Besombes and H. Boukari, Resonant optical pumping of a Mn spin in a strain-free quantum dot, Phys. Rev. B **89**, 085315 (2014).

[31] A. Lafuente-Sampietro, H. Boukari, and L. Besombes, Strain-induced coherent dynamics of coupled carriers and Mn spins in a quantum dot, Phys. Rev. B **92**, 081305 (2015).

[32] F. Tinjod, B. Gilles, S. Moehl, K. Kheng, and H. Mariette, II–VI quantum dot formation induced by surface energy change of a strained layer, Appl. Phys. Lett. **82**, 4340 (2003).

[33] M. Papaj, J. Kobak, J.-G. Rousset, E. Janik, M. Nawrocki, P. Kossacki, A. Golnik, and W. Pacuski, Photoluminescence studies of giant Zeeman effect in MBE-grown cobalt-based dilute magnetic semiconductors, J. Cryst. Growth **401**, 644 (2014).

[34] M. Papaj, J. Kobak, J.-G. Rousset, E. Janik, A. Golnik, P. Kossacki, and W. Pacuski, MBE growth and magnetooptical properties of (Zn,Co)Te layers, Acta Phys. Pol. A **122**, 1010 (2012).

[35] F. S. Ham, G. W. Ludwig, G. D. Watkins, and H. H. Woodbury, Spin Hamiltonian of Co^{2+}, Phys. Rev. Lett. **5**, 468 (1960).

[36] S.-Y. Wu and H.-N. Dong, On the EPR parameters of divalent cobalt in ZnX (X= S, Se, Te) and CdTe, Z. Naturforsch. **59**, 938 (2004).

[37] M. Grzybowski, A. Golnik, M. Sawicki, and W. Pacuski, Effect of magnetic field on intraionic photoluminescence of (Zn,Co)Se, Solid State Commun. **208**, 7 (2015).

[38] A. Lewicki, A. I. Schindler, I. Miotkowski, B. C. Crooker, and J. K. Furdyna, Specific heat of $Cd_{1-x}Co_xS$ and $Cd_{1-x}Co_xSe$ at low temperatures, Phys. Rev. B **43**, 5713 (1991).

[39] S. Isber, M. Averous, Y. Shapira, V. Bindilatti, A. N. Anisimov, N. F. Oliveira, V. M. Orera, and M. Demianiuk, Axial anisotropy of Co^{2+} in CdSe from the magnetization step and EPR, Phys. Rev. B **51**, 15211 (1995).

[40] V. Bindilatti, A. N. Anisimov, N. F. Oliveira, Y. Shapira, M. Goiran, F. Yang, S. Isber, M. Averous, and M. Demianiuk, Axial anisotropy of Co^{2+} in CdS from magnetization-step and high-frequency EPR, Phys. Rev. B **50**, 16464 (1994).

[41] T. Estle and M. De Wit, Paramagnetic resonance of Co^{2+} and V^{2+} in ZnO, Bull. Am. Phys. Soc. **6**, 445 (1961).

[42] R. M. Macfarlane, Perturbation methods in the calculation of Zeeman interactions and magnetic dipole line strengths for d^3 trigonal-crystal spectra, Phys. Rev. B **1**, 989 (1970).

[43] P. Koidl, Optical absorption of Co^{2+} in ZnO, Phys. Rev. B **15**, 2493 (1977).

[44] N. Jedrecy, H. J. von Bardeleben, Y. Zheng, and J.-L. Cantin, Electron paramagnetic resonance study of $Zn_{1-x}Co_xO$: A predicted high-temperature ferromagnetic semiconductor, Phys. Rev. B **69**, 041308 (2004).

[45] D. Ferrand, S. Marcet, W. Pacuski, E. Gheeraert, P. Kossacki, J. A. Gaj, J. Cibert, C. Deparis, H. Mariette, and C. Morhain, Spin carrier exchange interactions in (Ga,Mn)N and (Zn,Co)O wide band gap diluted magnetic semiconductor epilayers, J. Supercond. **18**, 15 (2005).

[46] P. Sati, R. Hayn, R. Kuzian, S. Régnier, S. Schäfer, A. Stepanov, C. Morhain, C. Deparis, M. Laügt, M. Goiran, and Z. Golacki, Magnetic Anisotropy of Co^{2+} as Signature of Intrinsic Ferromagnetism in ZnO:Co, Phys. Rev. Lett. **96**, 017203 (2006).

[47] W. Pacuski, D. Ferrand, J. Cibert, C. Deparis, J. A. Gaj, P. Kossacki, and C. Morhain, Effect of the s,p-d exchange interaction on the excitons in (Zn,Co)O epilayers, Phys. Rev. B **73**, 035214 (2006).

[48] X.-F. Yang, X.-S. Chen, W. Lu, and Y. Fu, Effects of shape and strain distribution of quantum dots on optical transition in the quantum dot infrared photodetectors, Nanoscale Res. Lett. **3**, 534 (2008).

[49] P. E. Vullum, M. Nord, M. Vatanparast, S. F. Thomassen, C. Boothroyd, R. Holmestad, B.-O. Fimland, and T. W. Reenaas, Quantitative strain analysis of InAs/GaAs quantum dot materials, Sci. Rep. **7**, 45376 (2017).